Enhancing the SEOBNRv5 effective-one-body waveform model with second-order gravitational self-force fluxes

Lorenzo Pompili

Max Planck Institute for Gravitational Physics (Albert Einstein Institute), Potsdam

arXiv:2303.18026, by M. van de Meent, A. Buonanno, D. Mihaylov, S. Ossokine, *L. Pompili*, N. Warburton, A. Pound, B. Wardell, L. Durkan, and J. Miller

arXiv:2303.18039, by *L. Pompili*, A. Buonanno, H. Estelles, M. Khalil, M. van de Meent, D. Mihaylov, S. Ossokine, M. Puerrer, A. Ramos-Buades et al.

26th Capra Meeting, Niels Bohr Institute (Copenhagen) July 5, 2023

Introduction

- More than 90 gravitational wave (GW) signals from compact binaries detected by LIGO and Virgo during their first three observing runs.

- Some signals (GW190412, GW190814) show evidence of mass asymmetry, and more are expected in the 4th observing run of the LIGO-Virgo-Kagra (LVK) collaboration: waveform models used for detecting and analyzing the GW signals need to be accurate in the small-mass-ratio (SMR) regime.

GW190412, [Abbott+, PRD 2020]

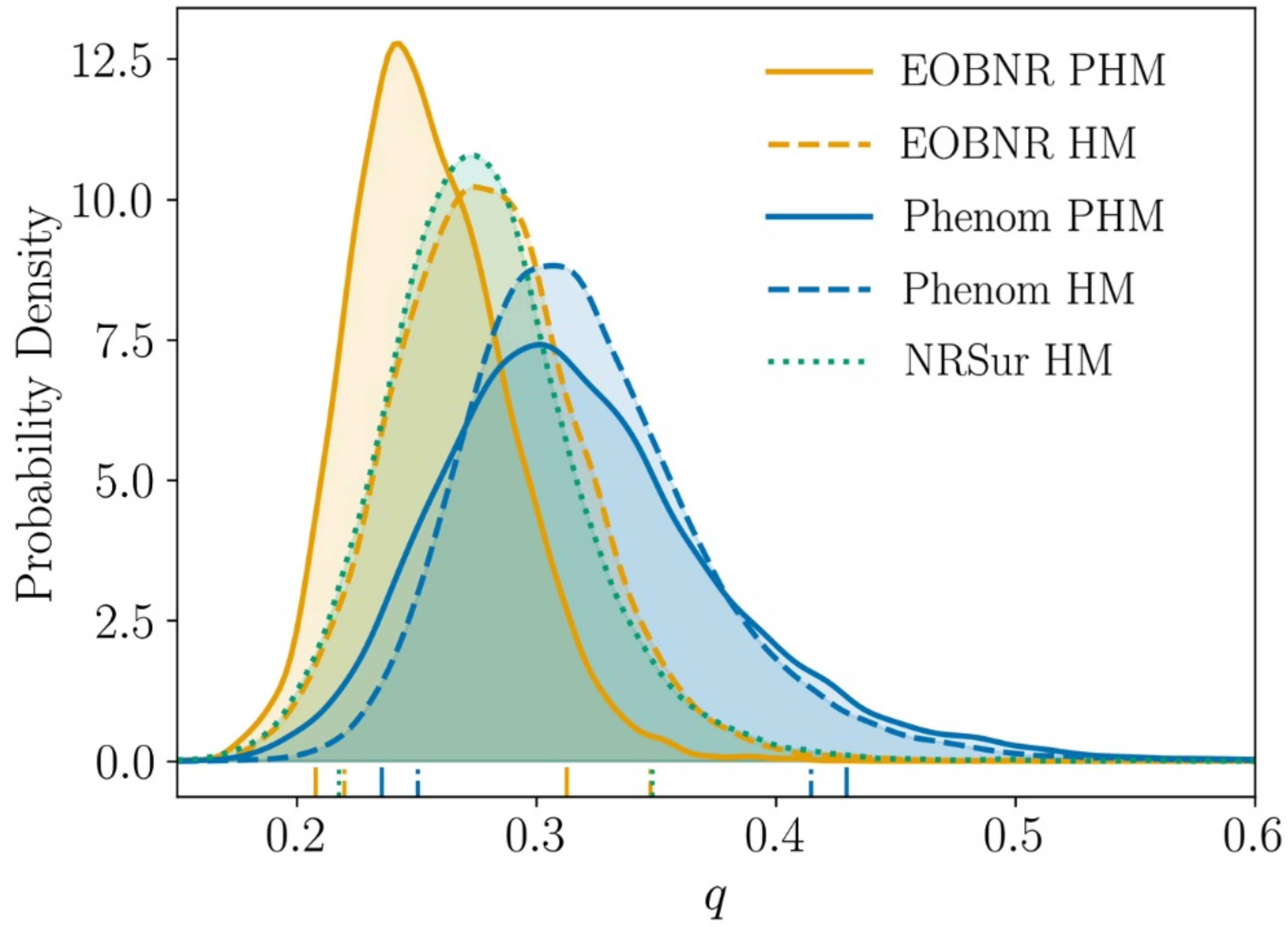

Introduction

- More than 90 gravitational wave (GW) signals from compact binaries detected by LIGO and Virgo during their first three observing runs.
- Some signals (GW190412, GW190814) show evidence of mass asymmetry, and more are expected in the 4th observing run of the LIGO-Virgo-Kagra (LVK) collaboration: waveform models used for detecting and analyzing the GW signals need to be accurate in the small-mass-ratio (SMR) regime.

GW190412, [Abbott+, PRD 2020]

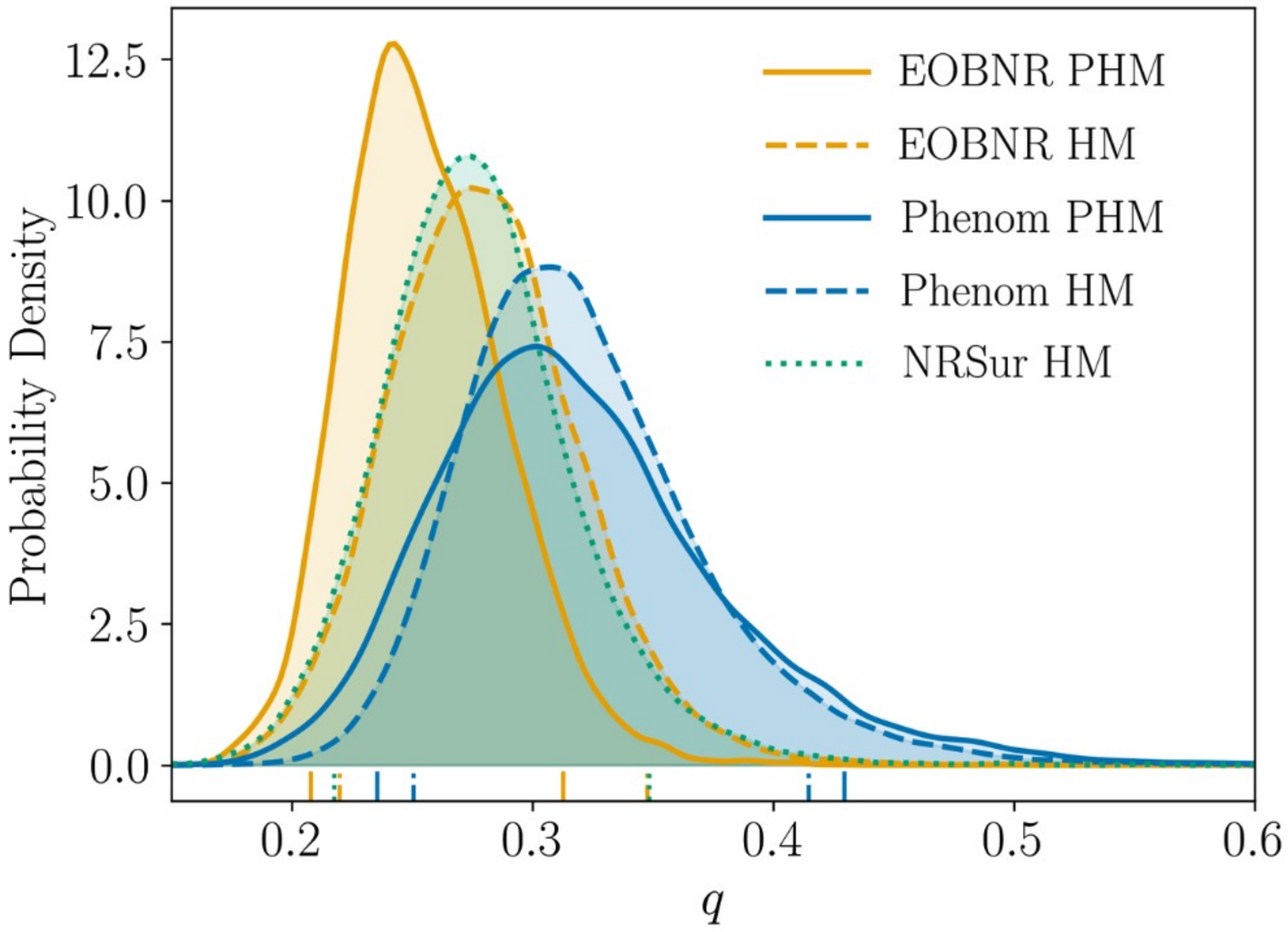

- Effective-one-body (EOB) theory provides accurate waveform models used for GW data analysis, combining resummed analytical results (e.g. from post-Newtonian (PN) theory) with numerical relativity (NR).
- EOB models reduce to the test-body motion around a black hole in the SMR limit: natural framework to incorporate results from SMR perturbation theory or gravitational self-force (GSF).

Introduction

Two main families of EOB models: SEOBNR and TEOBResumS. We focus on the latest generation of SEOBNR models for quasi-circular BBHs, SEOBNRv5 [Khalil+. 2023], [Pompili+, 2023], [Ramos-Buades+, 2023], [Van de Meent+, 2023].

- Several works on the inclusion of GSF results in the EOB waveforms and Hamiltonian (see e.g. [Damour, 2009], [Barausse+ 2012], [Le Tiec+, 2012], [Akcay+, 2012], [Akcay & Van de Meent, 2016], [Antonelli+, 2020], [Nagar & Albanesi, 2022]), as well as detailed comparisons within the TEOBResumS family [Albertini+, 2022].

Introduction

Two main families of EOB models: SEOBNR and TEOBResumS. We focus on the latest generation of SEOBNR models for quasi-circular BBHs, SEOBNRv5 [Khalil+. 2023], [Pompili+, 2023], [Ramos-Buades+, 2023], [Van de Meent+, 2023].

- Several works on the inclusion of GSF results in the EOB waveforms and Hamiltonian (see e.g. [Damour, 2009], [Barausse+ 2012], [Le Tiec+, 2012], [Akcay+, 2012], [Akcay & Van de Meent, 2016], [Antonelli+, 2020], [Nagar & Albanesi, 2022]), as well as detailed comparisons within the TEOBResumS family [Albertini+, 2022].

- Recent breakthrough calculations have provided the second-order GSF (2GSF) correction to the energy flux [Warburton+, 2021] as well as corresponding post-adiabatic waveforms [Wardell+, 2021].

- In this work we incorporate 2GSF energy flux corrections in the SEOBNRv5HM gravitational-mode amplitudes and radiation-reaction (RR) force. Including these corrections improves the waveform model both at small mass-ratios and for comparable masses.

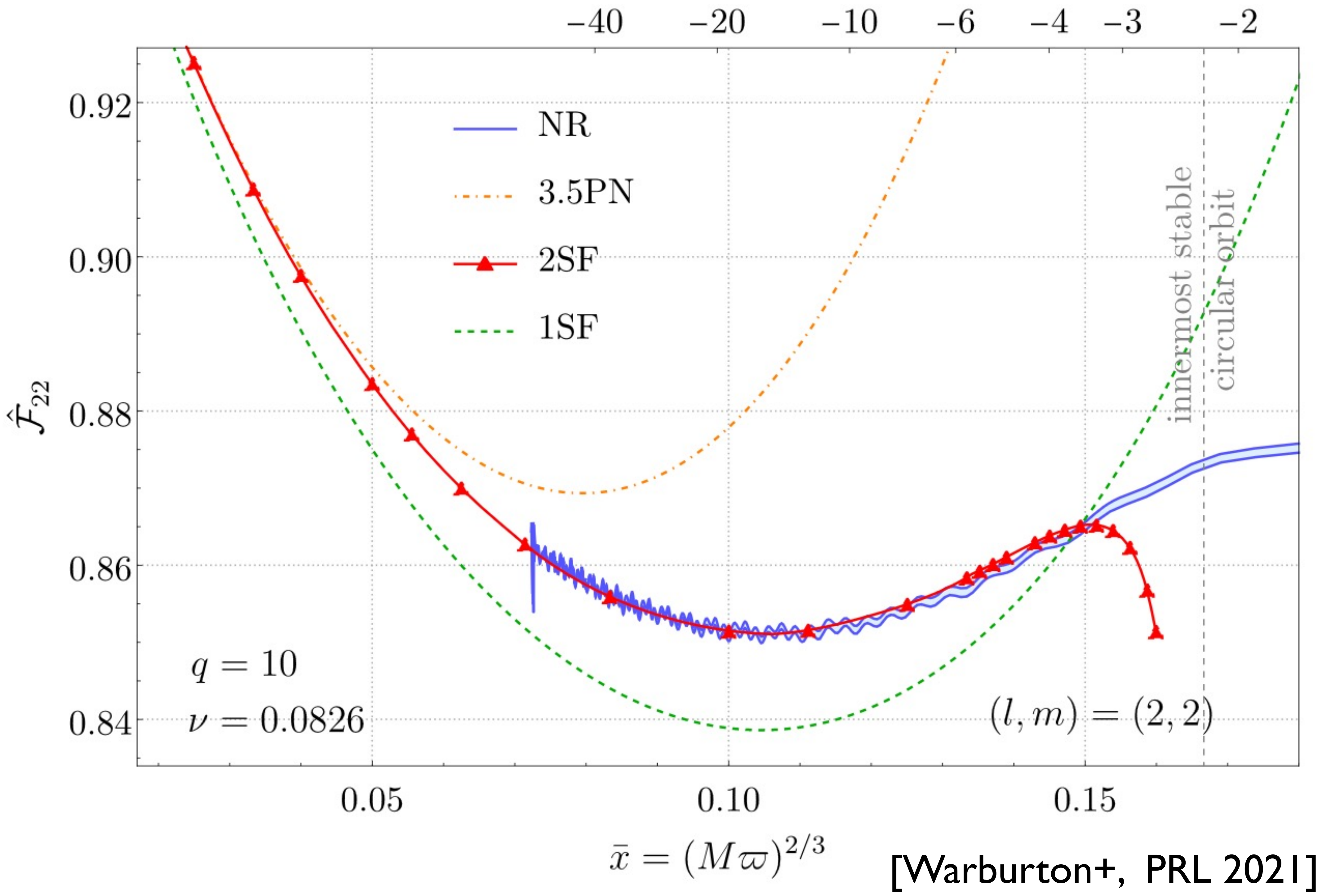

[Warburton+, PRL 2021]

The EOB Hamiltonian

- The Hamiltonian H_{EOB} describing the conservative binary dynamics is related to the effective Hamiltonian H_{eff} describing the dynamics of a test body in a deformed BH background, via the energy map

$$H_{\mathrm{EOB}} = M\sqrt{1 + 2\nu\left(\frac{H_{\mathrm{eff}}}{\mu} - 1\right)}$$

$$M = m_1 + m_2$$
$$\mu = m_1 m_2 / M$$
$$\nu = \mu / M$$

The EOB Hamiltonian

- The Hamiltonian H_{EOB} describing the conservative binary dynamics is related to the effective Hamiltonian H_{eff} describing the dynamics of a test body in a deformed BH background, via the energy map

$$H_{\mathrm{EOB}} = M\sqrt{1 + 2\nu\left(\frac{H_{\mathrm{eff}}}{\mu} - 1\right)}$$

$$M = m_1 + m_2$$
$$\mu = m_1 m_2 / M$$
$$\nu = \mu / M$$

- For nonspinning binaries H_{eff} reduces to the Hamiltonian of a test mass in a Schwarzschild background in the $\nu \to 0$ limit. Currently known at 4PN with partial results at 5PN and 6PN.

$$H_{\mathrm{eff}} = \sqrt{p_{r_*}^2 + A(r)\left[\mu^2 + \frac{p_\phi^2}{r^2} + Q\left(r, p_{r_*}\right)\right]}$$

The EOB Hamiltonian

- The Hamiltonian $H_{\rm EOB}$ describing the conservative binary dynamics is related to the effective Hamiltonian $H_{\rm eff}$ describing the dynamics of a test body in a deformed BH background, via the energy map

$$H_{\rm EOB} = M\sqrt{1 + 2\nu\left(\frac{H_{\rm eff}}{\mu} - 1\right)}$$

$$M = m_1 + m_2$$
$$\mu = m_1 m_2 / M$$
$$\nu = \mu / M$$

- For nonspinning binaries $H_{\rm eff}$ reduces to the Hamiltonian of a test mass in a Schwarzschild background in the $\nu \to 0$ limit. Currently known at 4PN with partial results at 5PN and 6PN.

$$H_{\rm eff} = \sqrt{p_{r_*}^2 + A(r)\left[\mu^2 + \frac{p_\phi^2}{r^2} + Q\left(r, p_{r_*}\right)\right]}$$

$$A(r) = 1 - \frac{2}{r} + \frac{2\nu}{r^3} + \nu\left(\frac{94}{3} - \frac{41\pi^2}{32}\right)\frac{1}{r^4} + \frac{a_5}{r^5} + \left[\nu\, a_6 + \nu\left(\frac{144\nu}{5} + \frac{7004}{105}\right)\ln r\right]\frac{1}{r^6}$$

unknown 5PN coefficient calibrated to NR

GW modes and radiation-reaction

GW polarizations and modes : $h = h_+ - i h_\times = \sum_{\ell=2}^{\infty} \sum_{m=-\ell}^{\ell} {}_{-2}Y_{\ell m}\left(\iota, \varphi_0\right) h_{\ell m}(t)$

EOB GW modes resum the PN-expanded GW modes in a factorized form: $h^F_{\ell m} = h^{\rm Newt}_{\ell m} \hat{S}_{\ell m} T_{\ell m} (\rho_{\ell m})^\ell e^{i \delta_{\ell m}}$

GW modes and radiation-reaction

GW polarizations and modes : $h = h_+ - ih_\times = \sum_{\ell=2}^{\infty} \sum_{m=-\ell}^{\ell} {}_{-2}Y_{\ell m}\left(\iota, \varphi_0\right) h_{\ell m}(t)$

EOB GW modes resum the PN-expanded GW modes in a factorized form: $h^F_{\ell m} = h^{\rm Newt}_{\ell m} \hat{S}_{\ell m} T_{\ell m} (\rho_{\ell m})^\ell e^{i\delta_{\ell m}}$

EOB energy flux: $\mathscr{F}^{\rm EOB} = \sum_{\ell=2}^{8} \sum_{m=1}^{\ell} \mathscr{F}^{\rm EOB}_{\ell m} = \sum_{\ell=2}^{8} \sum_{m=1}^{\ell} d_L^2 \frac{(mM\Omega)^2}{8\pi} \left| h^F_{\ell m} \right|^2$

GW modes and radiation-reaction

GW polarizations and modes : $h = h_+ - ih_\times = \sum_{\ell=2}^{\infty} \sum_{m=-\ell}^{\ell} {}_{-2}Y_{\ell m}\left(\iota, \varphi_0\right) h_{\ell m}(t)$

EOB GW modes resum the PN-expanded GW modes in a factorized form: $h^F_{\ell m} = h^{\rm Newt}_{\ell m} \hat{S}_{\ell m} T_{\ell m} (\rho_{\ell m})^\ell e^{i\delta_{\ell m}}$

EOB energy flux: $\mathcal{F}^{\rm EOB} = \sum_{\ell=2}^{8} \sum_{m=1}^{\ell} \mathcal{F}^{\rm EOB}_{\ell m} = \sum_{\ell=2}^{8} \sum_{m=1}^{\ell} d_L^2 \frac{(mM\Omega)^2}{8\pi} \left| h^F_{\ell m} \right|^2$

2GSF energy flux: $\mathcal{F}^{\rm GSF}_{\ell m}(\nu) = \nu^2 \mathcal{F}^{\rm GSF1}_{\ell m} + \nu^3 \mathcal{F}^{\rm GSF2}_{\ell m} + \mathcal{O}\left(\nu^4\right),$

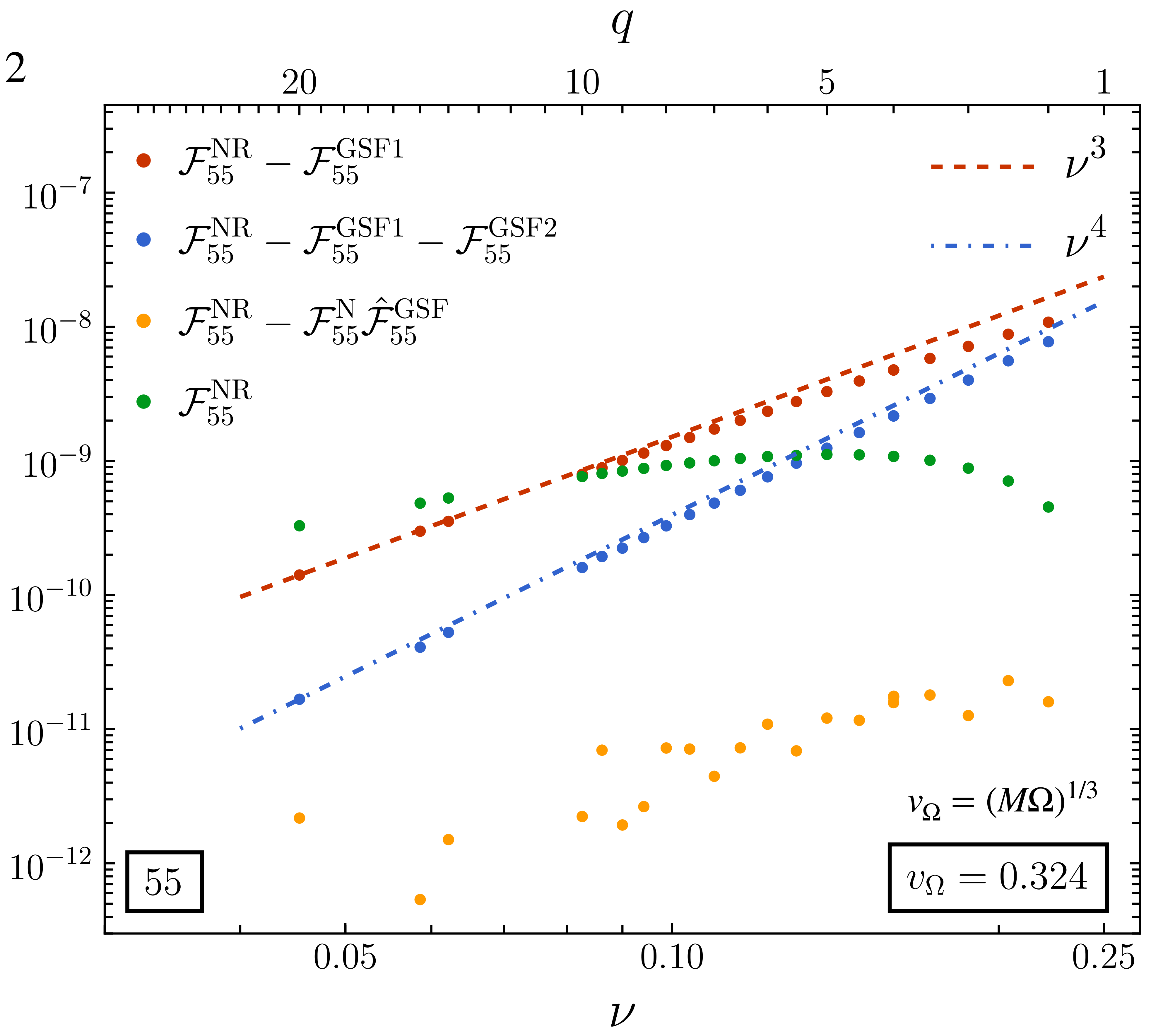

Re-expanded Newtonian-normalized flux:

$$\frac{\mathcal{F}^{\rm GSF}_{\ell m}}{\mathcal{F}^{\rm N}_{\ell m}} = \hat{\mathcal{F}}^{\rm GSF1}_{\ell m} + \nu \hat{\mathcal{F}}^{\rm GSF2}_{\ell m} + \mathcal{O}\left(\nu^2\right) = \hat{\mathcal{F}}^{\rm GSF}_{\ell m} + \mathcal{O}\left(\nu^2\right)$$

Matching the EOB and GSF multipolar fluxes

To incorporate information from the 2GSF flux in the EOB flux, we compare the respective (ℓ, m) mode Newtonian-normalized fluxes at a fixed value of the orbital frequency $M\Omega$.

Since the GSF result is given as an expansion in powers of ν, we need to do the same with the EOB energy fluxes: $\hat{\mathcal{F}}^{\rm EOB}_{\ell m} = \left|\hat{S}_{\ell m}\right|^2 \left|T_{\ell m}\right|^2 \left|\rho_{\ell m}\right|^{2\ell}$

Matching the EOB and GSF multipolar fluxes

To incorporate information from the 2GSF flux in the EOB flux, we compare the respective (ℓ, m) mode Newtonian-normalized fluxes at a fixed value of the orbital frequency $M\Omega$.

Since the GSF result is given as an expansion in powers of ν, we need to do the same with the EOB energy fluxes: $\hat{\mathcal{F}}^{\rm EOB}_{\ell m} = \left|\hat{S}_{\ell m}\right|^2 \left|T_{\ell m}\right|^2 \left|\rho_{\ell m}\right|^{2\ell}$

Expanding the individual factors and matching the expressions order-by-order in ν we can fix

$$\rho^{(0),\rm GSF}_{\ell m} = \left(\frac{\hat{\mathcal{F}}^{\rm GSF1}_{\ell m}}{\mathcal{T}^{(0)}_{\ell m}\left|\hat{S}^{(0)}_{\ell m}\right|^2}\right)^{1/(2\ell)} \qquad \rho^{(1),\rm GSF}_{\ell m} = \frac{\rho^{(0)}_{\ell m}}{2\ell}\left(\frac{\hat{\mathcal{F}}^{\rm GSF2}_{\ell m}}{\hat{\mathcal{F}}^{\rm GSF1}_{\ell m}} - \frac{\mathcal{T}^{(1)}_{\ell m}}{\mathcal{T}^{(0)}_{\ell m}} - 2\frac{\hat{S}^{(1)}_{\ell m}}{\hat{S}^{(0)}_{\ell m}}\right).$$

Where $\rho_{\ell m} = \rho^{(0)}_{\ell m} + \nu\rho^{(1)}_{\ell m} + \mathcal{O}\left(\nu^2\right), \hat{S}_{\ell m} = \hat{S}^{(0)}_{\ell m} + \nu\hat{S}^{(1)}_{\ell m} + \mathcal{O}\left(\nu^2\right), \left|T_{\ell m}\right|^2 = \mathcal{T}^{(0)}_{\ell m} + \nu\mathcal{T}^{(1)}_{\ell m} + \mathcal{O}\left(\nu^2\right)$

Matching the EOB and GSF multipolar fluxes

To include 2GSF information in the EOB mode amplitudes we focus on the 7 dominant (ℓ, m) modes included in the SEOBNRv5HM model $(\ell, m) = (2,2), (2,1), (3,3), (3,2), (4,4), (4,3), (4,3)$. For each mode:

Matching the EOB and GSF multipolar fluxes

To include 2GSF information in the EOB mode amplitudes we focus on the 7 dominant (ℓ, m) modes included in the SEOBNRv5HM model $(\ell, m) = (2,2), (2,1), (3,3), (3,2), (4,4), (4,3), (4,3)$. For each mode:

- We determine the contributions to $\rho^{(1)}_{\ell m}$ already included in the EOB waveform by expanding $\rho_{\ell m}$ in powers of ν ($v_\Omega = (M\Omega)^{1/3}$).

$$\rho^{(1),\mathrm{EOB}}_{22} = \frac{55}{84} v_\Omega^2 - \frac{33025}{21168} v_\Omega^4 - \left[\frac{48993925}{9779616} - \frac{41\pi^2}{192}\right] v_\Omega^6$$

Matching the EOB and GSF multipolar fluxes

To include 2GSF information in the EOB mode amplitudes we focus on the 7 dominant (ℓ, m) modes included in the SEOBNRv5HM model $(\ell, m) = (2,2), (2,1), (3,3), (3,2), (4,4), (4,3), (4,3)$. For each mode:

- We determine the contributions to $\rho_{\ell m}^{(1)}$ already included in the EOB waveform by expanding $\rho_{\ell m}$ in powers of ν $(v_\Omega = (M\Omega)^{1/3})$.

$$\rho_{22}^{(1),\mathrm{EOB}} = \frac{55}{84}v_\Omega^2 - \frac{33025}{21168}v_\Omega^4 - \left[\frac{48993925}{9779616} - \frac{41\pi^2}{192}\right] v_\Omega^6$$

- We augment $\rho_{\ell m}^{(1),\mathrm{EOB}}$ with a polynomial $\Delta\rho_{\ell m}^{(1)}$ in v_Ω^2 starting at the lowest order not already included. $\Delta\rho_{\ell m}^{(1)}$ is determined by fitting to the numerical $\rho_{\ell m}^{(1),\mathrm{GSF}}$ results.

$$\Delta\rho_{22}^{(1)} = 21.2 v_\Omega^8 - 411 v_\Omega^{10}$$

Matching the EOB and GSF multipolar fluxes

To include 2GSF information in the EOB mode amplitudes we focus on the 7 dominant (ℓ, m) modes included in the SEOBNRv5HM model $(\ell, m) = (2{,}2), (2{,}1), (3{,}3), (3{,}2), (4{,}4), (4{,}3), (4{,}3)$. For each mode:

- We determine the contributions to $\rho^{(1)}_{\ell m}$ already included in the EOB waveform by expanding $\rho_{\ell m}$ in powers of ν ($v_\Omega = (M\Omega)^{1/3}$).

$$\rho^{(1),\mathrm{EOB}}_{22} = \frac{55}{84}v_\Omega^2 - \frac{33025}{21168}v_\Omega^4 - \left[\frac{48993925}{9779616} - \frac{41\pi^2}{192}\right] v_\Omega^6$$

- We augment $\rho^{(1),\mathrm{EOB}}_{\ell m}$ with a polynomial $\Delta\rho^{(1)}_{\ell m}$ in v_Ω^2 starting at the lowest order not already included. $\Delta\rho^{(1)}_{\ell m}$ is determined by fitting to the numerical $\rho^{(1),\mathrm{GSF}}_{\ell m}$ results.

$$\Delta\rho^{(1)}_{22} = 21.2 v_\Omega^8 - 411 v_\Omega^{10}$$

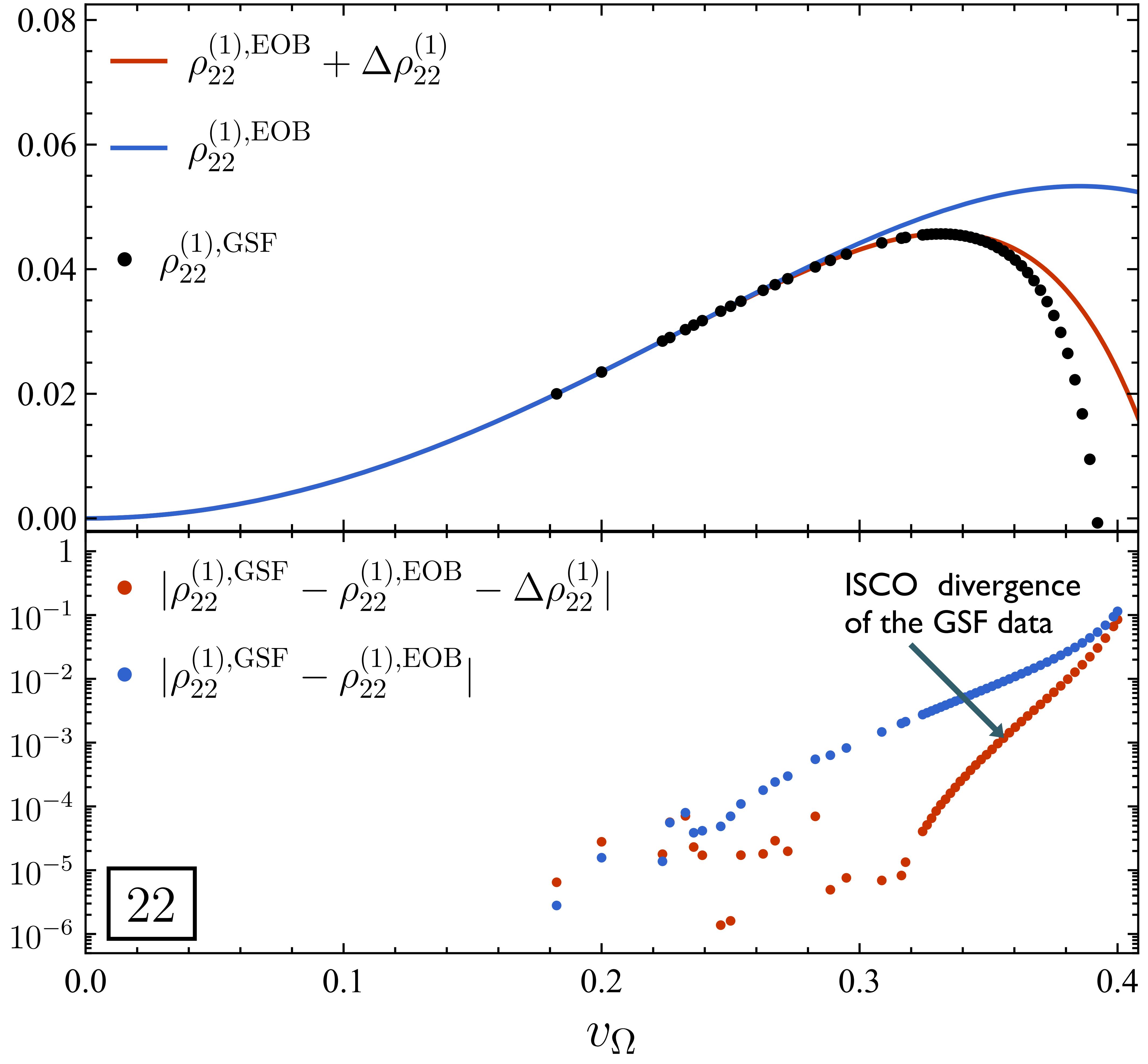

Impact on the model accuracy: energy fluxes

- We compare the energy flux of the SEOBNRv5HM model to the one extracted from a set of NR simulations ($1 \leq q \leq 20$) from the SXS collaboration.

- Even at modest mass-ratio, the 2GSF corrections improve the agreement with the NR flux by a factor of a few across all frequencies.

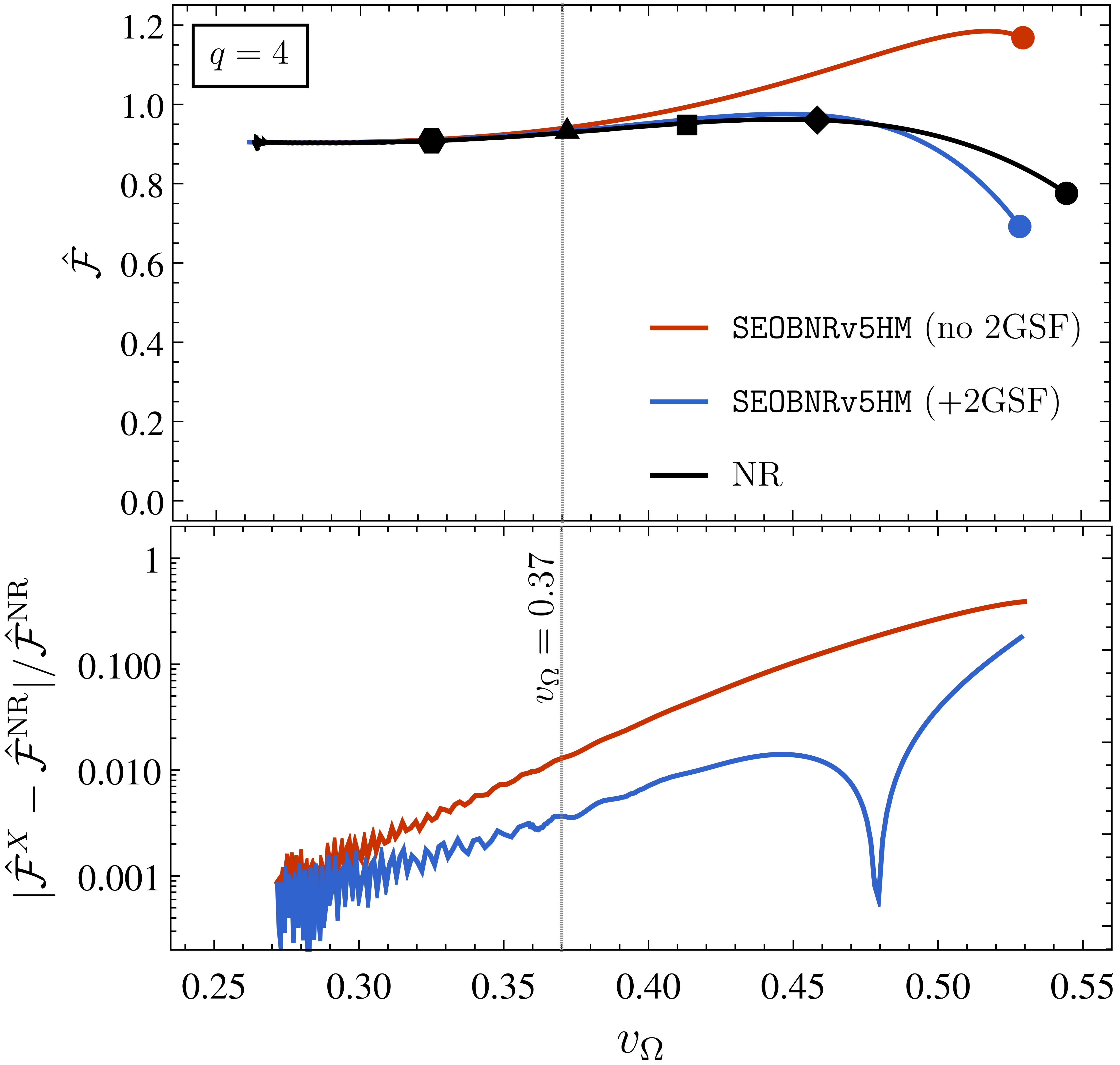

Impact on the model accuracy: energy fluxes

Relative error almost constant with ν (and not $\propto \nu^2$), possibly caused by

- Insufficient accuracy in the $\rho_{\ell m}^{(0),\mathrm{EOB}}$ (test-body flux).
- Corrections to the 2GSF flux from the transition to plunge starting to be relevant at $v_\Omega = 0.37$.

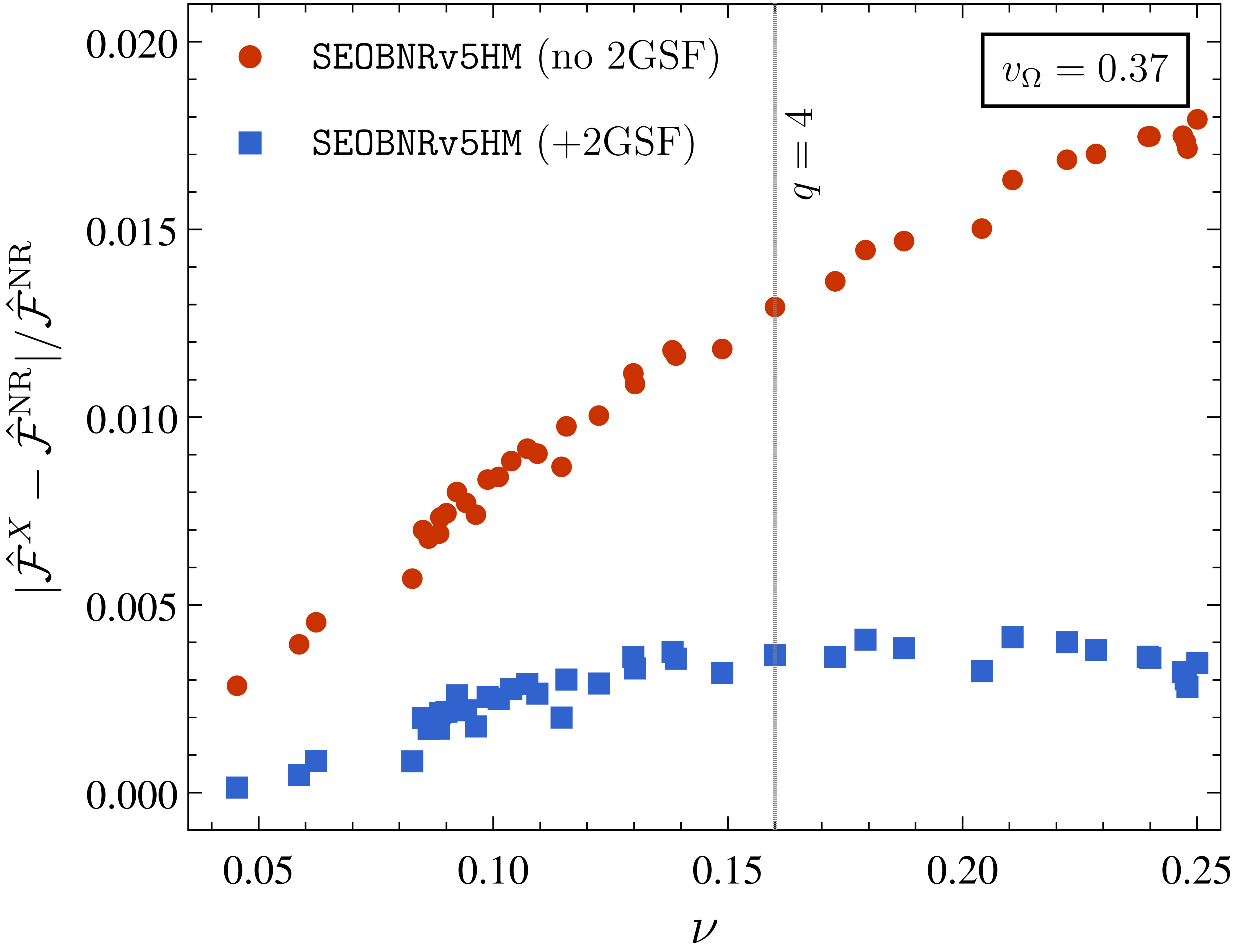

Impact on the model accuracy: mismatch

Mismatch between (2,2) mode of SEOBNRv5HM and NR waveforms, using the advanced LIGO noise curve.

$$\mathcal{M} = 1 - \max_{\delta\phi,\delta t} \frac{\left(h_{22}^{\mathrm{NR}} \mid h_{22}^{\mathrm{EOB}}\right)}{\sqrt{\left(h_{22}^{\mathrm{NR}} \mid h_{22}^{\mathrm{NR}}\right)\left(h_{22}^{\mathrm{EOB}} \mid h_{22}^{\mathrm{EOB}}\right)}} \qquad \left(h_1 \mid h_2\right) \equiv 4\,\mathrm{Re}\left[\int_{f_l}^{f_h} \frac{\tilde{h}_1(f)\tilde{h}_2^*(f)}{S_n(f)} \mathrm{d}f\right]$$

Impact on the model accuracy: mismatch

Mismatch between (2,2) mode of SEOBNRv5HM and NR waveforms, using the advanced LIGO noise curve.

$$\mathcal{M} = 1 - \max_{\delta\phi,\delta t} \frac{\left(h_{22}^{\rm NR} \mid h_{22}^{\rm EOB}\right)}{\sqrt{\left(h_{22}^{\rm NR} \mid h_{22}^{\rm NR}\right)\left(h_{22}^{\rm EOB} \mid h_{22}^{\rm EOB}\right)}} \qquad \left(h_1 \mid h_2\right) \equiv 4\,{\rm Re}\left[\int_{f_l}^{f_h} \frac{\tilde{h}_1(f)\tilde{h}_2^*(f)}{S_n(f)}{\rm d}f\right]$$

Both models with and without 2GSF corrections are calibrated to a subset of NR simulations. After calibration they show comparable mismatches:

- Mismatches between models and NR close to NR error (comparing highest and one lower NR resolution).
- Degeneracy between changes in the Hamiltonian and RR force: a different value of the calibration coefficient a_6 can compensate for imperfections in the dissipative sector.

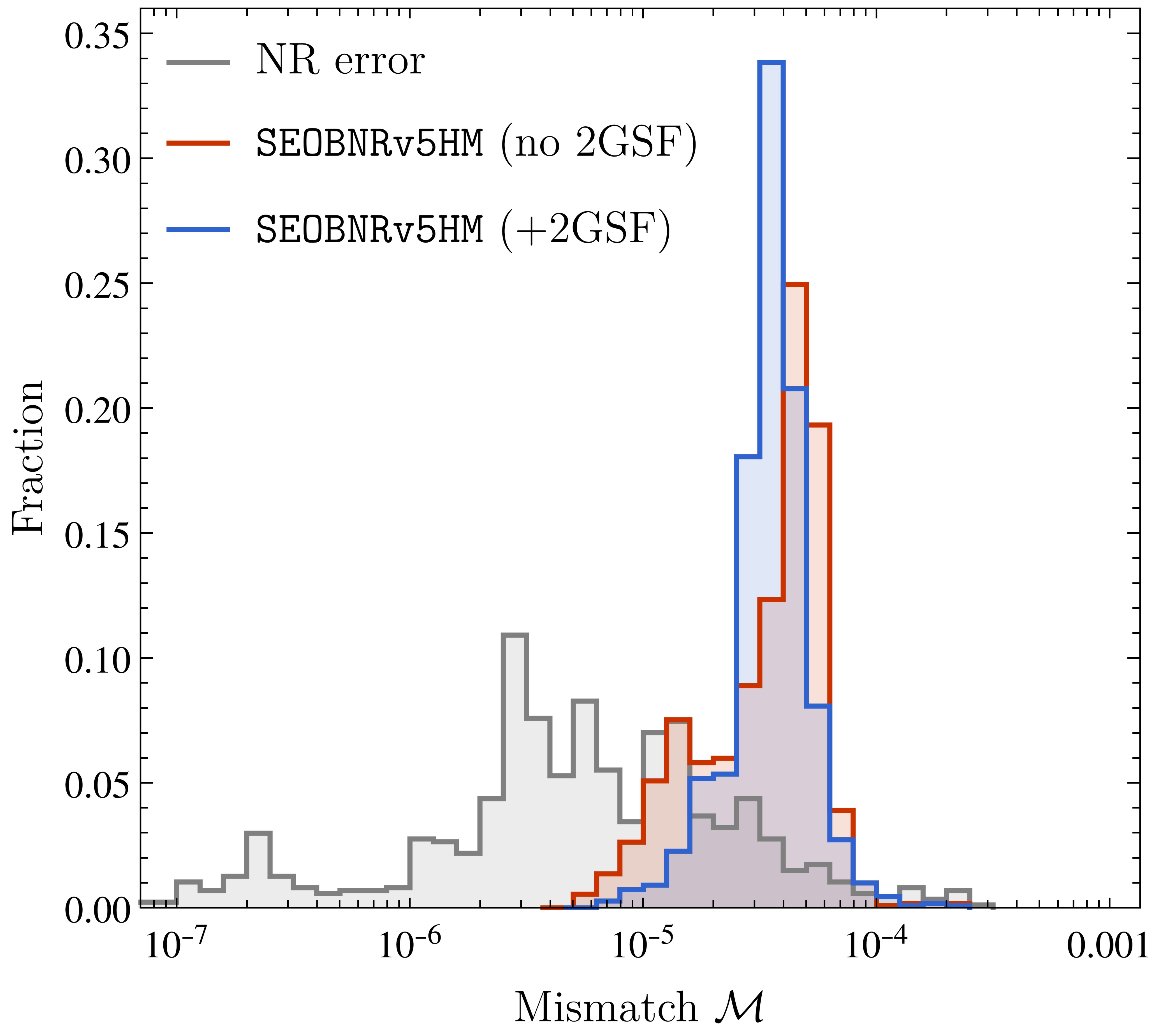

Impact on the model accuracy: binding energy

The SEOBNRv5HM models with and without 2GSF information have different Hamiltonians (due to a_6) and therefore differ in their binding energy $E_{\rm bind}^{\rm EOB} = H_{\rm EOB} - M$.

Impact on the model accuracy: binding energy

The SEOBNRv5HM models with and without 2GSF information have different Hamiltonians (due to a_6) and therefore differ in their binding energy $E_{\rm bind}^{\rm EOB} = H_{\rm EOB} - M$.

- We compare the SEOBNRv5HM binding energy to the one extracted from NR simulations: the model with 2GSF corrections reproduces the NR binding energy much more faithfully.
- The improvement persists even against aligned-spin binaries, despite only adding 2GSF corrections to the nonspinning part of the waveform and RR force.

Impact on the model accuracy: binding energy

The SEOBNRv5HM models with and without 2GSF information have different Hamiltonians (due to a_6) and therefore differ in their binding energy $E_{\rm bind}^{\rm EOB} = H_{\rm EOB} - M$.

- We compare the SEOBNRv5HM binding energy to the one extracted from NR simulations: the model with 2GSF corrections reproduces the NR binding energy much more faithfully.
- The improvement persists even against aligned-spin binaries, despite only adding 2GSF corrections to the nonspinning part of the waveform and RR force.

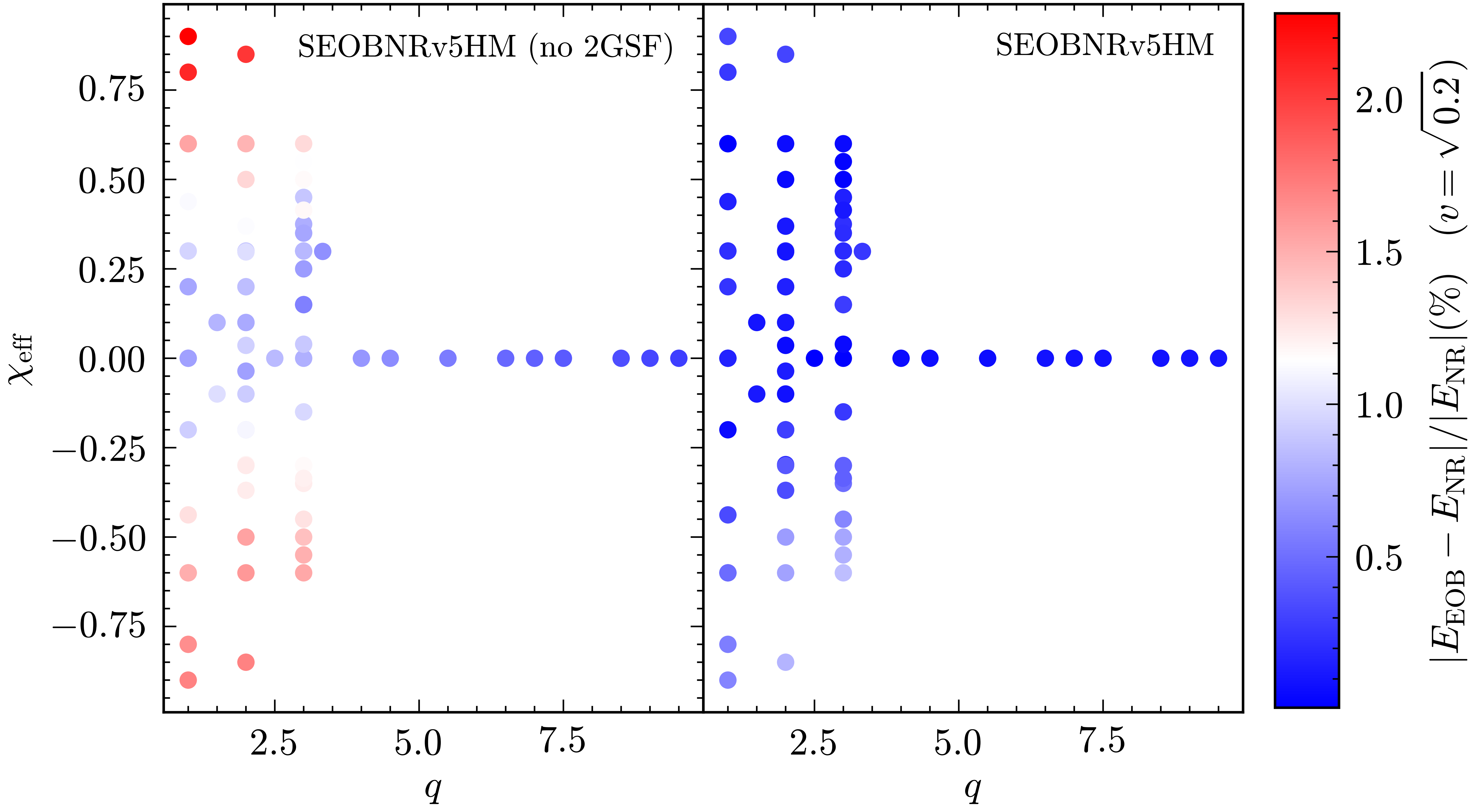

Conclusions

We have enhanced the accuracy of the factorized gravitational modes used in the SEORBNRv5 models by calibrating them to nonspinning, quasi-circular 2GSF multipolar data.

- Significant improvement in the faithfulness of the SEORBNRv5 flux compared to the one extracted from NR simulations.
- Marginal impact on the waveform mismatches against NR, due to degeneracies between changes in the dissipative and conservative dynamics.
- Significant improvement in the faithfulness of the SEOBNRv5 binding energy against NR, also for BBHs with spins. The improved consistency and naturalness of the model gives greater confidence that it will remain faithful to NR when extrapolated beyond the calibration region, in particular for higher mass ratios.

Conclusions

Possible extensions of this work:

- The matching procedure employed here could be used to calibrate the SEOBNRv5HM modes to data that include corrections to the 2GSF flux linear in either the primary or secondary spin.
- The 2GSF flux data we used do not include corrections due to the transition from inspiral to plunge, so it diverges at the ISCO. Including these terms could lead to further improvements of our results in the strong-field regime.

SEOBNRv5 models publicly available through the python package `pyseobnr`

git.ligo.org/waveforms/software/pyseobnr

Backup Slides

Waveform comparisons